AIMS Microbiology, 12(4): 815–839.
DOI: 10.3934/microbiol.2026035
Received: 07 August 2026
Revised: 16 October 2026
Accepted: 27 October 2026
Published: 3 November 2026

https://www.aimspress.com/journal/microbiology

Research article

Genomic epidemiology and plasmid architecture of linezolid-resistant *Enterococcus faecium* in a Czech tertiary-care hospital

Holubova Ema[1,2], Jakubickova Marketa[1,2,3], Bezdicek Matej[1,2,4], Bitusikova Viktoria[1,2], Vitkova Helena[3], Kocmanova Iva[1,2], Vitkova Ivana[1], Kubackova Petra[1], Kabut Tomas[4,5], Weinbergerova Barbora[4,5], Hodova Silvie[6], Zdrazilova-Dubska Lenka[1,2] and Lengerova Martina[1,2,4,*]

[1] Division of Clinical Microbiology and Immunology, Department of Laboratory Medicine, University Hospital Brno, Brno, Czech Republic
[2] Division of Clinical Microbiology and Immunology, Department of Laboratory Medicine, Faculty of Medicine, Masaryk University, Brno, Czech Republic
[3] Department of Biomedical Engineering, Faculty of Electrical Engineering and Communication, Brno University of Technology, Brno, Czech Republic
[4] Department of Internal Medicine—Hematology and Oncology, Masaryk University, Brno, Czech Republic
[5] Department of Internal Medicine—Hematology and Oncology, University Hospital Brno, Brno, Czech Republic
[6] Department of Infection Control and Hospital Hygiene, University Hospital Brno, Brno, Czech Republic

* **Correspondence:** Email: lengerova.martina@fnbrno.cz; Tel: +420532234629.

Abstract: Linezolid-resistant *Enterococcus faecium* represents an increasing challenge in healthcare settings. We characterized 75 isolates initially identified as linezolid resistant from 64 patients at a Czech tertiary-care hospital between June 2022 and June 2024 using Oxford Nanopore whole-genome sequencing, genomic typing, core-genome SNV analysis, and plasmid reconstruction. Eight sequence types were identified, dominated by ST1192 (45.3%) and ST7 (40.0%). ST1192 formed a highly homogeneous cluster (0–6 SNVs), whereas ST7 showed greater overall diversity (0–74 SNVs), although most ST7 isolates remained closely related (median pairwise distance: 1 SNV). Confirmatory linezolid MICs ranged from 4 to 256 mg/L; 73 isolates were resistant and 2 were susceptible according to EUCAST breakpoints. All isolates carried the 23S rRNA G2576T mutation, while no acquired linezolid-resistance genes were detected. ST1192 isolates had significantly higher linezolid MICs and

G2576T mutant allele frequencies than ST7 isolates. Five plasmid clusters carried antimicrobial resistance or putative virulence determinants, including a widely distributed pELF-like plasmid harboring the *vanA* resistance gene cluster. This plasmid was highly prevalent across both dominant lineages but exhibited structural variation associated with partial or complete duplications. These findings demonstrate prolonged circulation of two predominant G2576T-positive lineages and a broadly conserved plasmid repertoire, highlighting the value of long-read sequencing for integrated surveillance of chromosomal resistance and plasmid architecture in hospital-associated *E. faecium*.

Keywords: *Enterococcus faecium*; linezolid resistance; whole-genome sequencing; genomic epidemiology; plasmids

1. Introduction

Enterococcus faecium is a Gram-positive coccus belonging to the lactic acid bacteria group and can survive harsh environmental conditions, including elevated temperatures and alkaline pH [1]. The species exhibits substantial genetic diversity and frequently harbors plasmids that facilitate dissemination of antimicrobial-resistance determinants [2–4]. Plasmids may also disseminate adaptive traits associated with colonization, persistence, and survival in hospital environments [4]. Over recent decades, *E. faecium* has emerged as a major nosocomial pathogen, with vancomycin and linezolid resistance posing significant therapeutic challenges [1,5,6].

Linezolid resistance in *E. faecium* is mediated by several mechanisms. The most common is the G2576T substitution in the 23S rRNA gene, which is frequently associated with multidrug-resistant phenotypes [6,7]. Among plasmid-borne determinants, *optrA* confers transferable resistance to linezolid, phenicols, and tetracyclines [8]. Another ABC-F family member, *poxtA*, often co-occurs with *optrA* on plasmids and may be flanked by IS*1216E* elements that facilitate horizontal transfer [9]. Although *poxtA* alone does not always confer high-level resistance, it contributes to reduced susceptibility and has been detected in diverse clinical and environmental isolates [9]. Less frequently, *cfr* and mutations in the ribosomal protein genes *rplC*, *rplV*, and *rplD* have been implicated in resistance development [7].

Beyond linezolid resistance, plasmids contribute to the adaptation and persistence of *E. faecium* in hospital environments [4]. Studies have described pELF-type linear plasmids carrying resistance and metabolic determinants that may facilitate colonization, persistence, and dissemination of hospital-adapted lineages [4].

Our aim of this study was to characterize the population structure, resistance mechanisms, and plasmid architecture of linezolid-resistant *E. faecium* (LREfm) isolates collected over a two-year period in a Czech tertiary-care hospital. Using Oxford Nanopore long-read whole-genome sequencing and the introduced MLST scheme, we sought to elucidate clonal dynamics, transmission patterns, chromosomal mechanisms of linezolid resistance, and the distribution of resistance- and virulence-associated plasmids within the hospital population.

2. Methods

2.1. Bacterial isolates and patients

Between June 2022 and June 2024, routine screening and clinical diagnostic testing identified 75 *E. faecium* isolates that were initially reported as linezolid-resistant by routine antimicrobial susceptibility testing. Confirmatory linezolid MIC testing subsequently classified 73 isolates as resistant and 2 isolates as susceptible according to EUCAST clinical breakpoints (v15.0).

Most isolates (n = 65) originated from the Department of Internal Medicine—Hematology and Oncology. The remaining 10 isolates were recovered from patients hospitalized at the Department of Gastroenterology and Internal Medicine (n = 4), Clinic of Anaesthesiology, Resuscitation and Intensive Medicine (n = 4), Department of Infectious Diseases (n = 1), and Department of Internal Medicine and Cardiology (n = 1). The isolates were obtained predominantly from rectal swabs (n = 40), urine (n = 11), and stool samples (n = 10), followed by respiratory tract secretions (n = 3), blood cultures (n = 2), bronchoalveolar lavage fluid (n = 1), sputum (n = 1), and other swabs (n = 7). Rectal swabs (n = 40; 53.3%) were collected as part of routine screening, whereas the remaining 35 isolates (46.7%) were recovered from specimens submitted for clinical diagnostic testing. Species identification was performed using MALDI-TOF mass spectrometry. Confirmatory linezolid and vancomycin MICs were determined using MIC Test Strips (linezolid, 0.016–256 mg/L; vancomycin, 0.016–256 mg/L; Liofilchem s.r.l., Italy) and interpreted according to the applicable EUCAST clinical breakpoints. Relevant clinical information, including the timing and duration of linezolid treatment, was retrospectively retrieved from hospital records. Although treatment timing and duration were available from clinical records, this exploratory analysis classified exposure only as a binary variable according to whether linezolid treatment occurred before isolate collection and did not model cumulative dose or treatment duration.

2.1.1. DNA isolation and whole genome sequencing

Genomic DNA was extracted using the DNeasy PowerSoil Pro Kit (Qiagen, Netherlands) according to the manufacturer's instructions. Sequencing libraries were prepared with the Rapid Barcoding Kit V14 and sequenced on the PromethION 2 Solo platform using R10.4.1 flow cell chemistry (Oxford Nanopore Technologies, UK).

2.1.2. Bioinformatics data processing and computational downstream analysis

Raw sequencing data were basecalled using Dorado integrated in MinKNOW (v23.11.5, nanoporetech.com/community) with the super-accurate basecalling model (dna r10.4.1 e8.2 400bps sup@v5.0.0). Reads with a minimum quality score of 10 were retained for further analysis. Adapter trimming was performed using Dorado (v1.3.1, github.com/nanoporetech/dorado), which was also used for read demultiplexing. To remove potential host-derived contamination, trimmed reads were mapped to the human genome (GCF 000001405.40) by minimap2 (v2.28) [10]. Unmapped reads were extracted by Samtools (v1.10) and then genome de novo assembly was performed by an Autocycler (v0.6.2) [11] as follows: Approximate genome size was first estimated using Raven and then the reads were randomly subsampled into four individual subsets. Each subset was assembled

using Flye (v2.9.6) [12], Miniasm (v0.3) [13], and Raven (v1.8.3) [14]. The resulting assemblies were combined into a unitig graph and grouped into clusters representing putative replicons. Clusters that passed quality control were trimmed to remove overlapping end regions and resolved into consensus sequences. Some replicons were not resolved as circular, suggesting the presence of linear plasmids, so these fragmented components were manually curated by selecting the best-supported candidate sequence based on read coverage depth, completeness, and evenness across the sequence. Finally, all resolved clusters were combined to generate the final genome assembly of each isolate. Sequencing and assembly metrics for each isolate, including the number of trimmed reads retained after host-contamination removal, mean read length, total assembly length, contig and chromosome counts, number of plasmids, circular and linear contig counts, and estimated coverage, are provided in Table S1.

In each obtained assembly, the contigs were classified by lengths. The largest contig, which had approximately 2.7 Mbp, was labeled as chromosome, and the non-chromosomal contigs were considered candidate plasmids based on their size, assembly topology, presence of plasmid-associated features, or similarity to known plasmids.

MLST and cgMLST analyses were performed using Ridom SeqSphere+ software (v10.0.5) with the incorporated schemes. The original MLST scheme [15] and the scheme proposed by Bezdíček et al. [16] comprised 7 and 8 loci, respectively, whereas the *E. faecium* cgMLST scheme comprised 1,423 core-genome targets. Isolates were assigned sequence types according to both MLST schemes, which are available through the PubMLST database.

To identify SNPs, the obtained assemblies were aligned using Snippy (v4.6.0) [17] against reference genome NC_017022.2, which was used as a seed genome for *E. faecium* cgMLST. The cgSNP alignment was built with snippy-core, and pairwise SNV distances calculated from this alignment were used to construct a minimum spanning tree (MST) using Kruskal's algorithm [18]. The MST was visualized using Cytoscape (v3.10.4) [19].

To mitigate the impact of sequencing errors inherent to long-read data, high-accuracy basecalling models were applied, and SNV-based analyses were interpreted conservatively, focusing on broader genetic distance patterns rather than single-SNV differences.

The assembled genomes were screened for antimicrobial resistance and virulence genes using ResFinder (v4.6.0) and VirulenceFinder (v3.0.1) tools [20,21]. Linezolid resistance-associated mutations, specifically G2576T and G2505A in the 23S rRNA gene, were detected and quantified from quality-filtered, host-depleted sequencing reads using LRE-Finder (v1.0) [22]. Mutant allele frequencies were calculated from the proportion of sequencing reads carrying the respective mutation. For descriptive purposes, an approximate number of 23S rRNA gene copies carrying the G2576T mutation was derived from the observed mutant allele frequency, assuming six 23S rRNA gene copies per genome. The mutant allele frequency was multiplied by 6 and divided by 100, and the resulting value was rounded up to the nearest whole number. This ceiling-based value was treated as an estimated copy-number category rather than a directly measured number of mutated gene copies. All statistical analyses were therefore based on the observed G2576T mutant allele frequency rather than on the derived copy-number estimate.

In addition, BLAST searches (v2.12) were performed to identify plasmid-mediated resistance gene presence [23], including *optrA* (NG_048023), *poxtA* (NG_063824.1), *poxtA-Ef* (NG_081674.1), *cfrB* (NG_050395.1), and *cfrD* (NG_067192.1). Mutations in ribosomal protein genes *rplC*, *rplD*, and *rplV* were investigated using wild-type reference sequences from the CP003583.1 genome [24].

The contigs labeled plasmids were clustered using PlasTree (v0.1.3) [25], where all 3 modules (--methods dotplot kmer pang) were used. As the pang method requires pangenome results, the plasmid sequences were first annotated by Bakta (v1.12.0) [26], and the obtained annotations were used to establish a pangenome using Panaroo (v1.7.0) [27]. The resulting PlasTree consensus tree was cut at a maximum branch length of 0.2 to define plasmid clusters. For each plasmid sequence, its mobility was determined using MOB-suite (v3.1.9) [28].

Tn*1546-like* elements were characterized in all 70 plasmids carrying the *vanHAX* gene cluster. Each plasmid sequence was compared with the reference Tn*1546* sequence (GenBank M97297.1) using BLASTn (v2.17.0) with an e-value threshold of 1e-10 [23,29]. Structural differences were recorded relative to the reference coordinates, including deletions, insertions, and nucleotide substitutions. A gene was considered complete when its sequence was contained in a single continuous alignment with at least 95% nucleotide identity. Insertion sequences were identified using ISfinder, retaining hits with at least 90% identity over at least 80% of the IS length [30]. Elements with identical deletion and insertion-sequence patterns were grouped into structural profiles based on the complete Tn*1546*-like element in each plasmid.

For contextual analysis, 3,278 publicly available *E. faecium* genomes were retrieved from the PubMLST database. Available metadata included the country and year of isolation, source category, source, and sequence type according to the original and recently introduced MLST schemes (Supplementary Data S1).

2.1.3. Statistical analysis

Statistical analyses were performed to evaluate differences in linezolid minimum inhibitory concentrations (MICs) and G2576T mutant allele frequencies between groups of *E. faecium* isolates. Continuous variables were summarized using medians and interquartile ranges (IQRs). Because the distributions were non-normal, as assessed by visual inspection, non-parametric methods were used throughout. Comparisons between two independent groups, including isolates obtained from patients with and without documented linezolid treatment before sampling and comparisons between sequence types, were performed using two-sided Mann–Whitney U tests. Effect sizes for selected comparisons were estimated using the Hodges–Lehmann estimator with corresponding 95% confidence intervals (CIs). The association between G2576T mutant allele frequency and linezolid MIC was assessed using Spearman's rank correlation coefficient. Correlations were calculated for the complete isolate collection and separately for the two predominant sequence types, ST7 and ST1192, to determine whether the overall association persisted within individual lineages.

Primary analyses were performed at the isolate level. Because 11 of the 75 isolates were additional isolates from patients already represented in the collection, a sensitivity analysis was conducted using only the first chronologically collected isolate from each patient (n = 64). Treatment-related comparisons of linezolid MICs and G2576T mutant allele frequencies were repeated in this patient-level sensitivity dataset. A p-value < 0.05 was considered statistically significant. Given the exploratory nature of the study and the small sample sizes in some subgroup analyses, no correction for multiple comparisons was applied. The results were therefore interpreted cautiously, with emphasis on effect sizes and overall patterns. Statistical analyses were performed in R (version 4.6.1) using the custom script provided as Supplementary Code S1.

3. Results

3.1. WGS-based typing

In total, 8 distinct STs were identified, with the population dominated by 2 major clonal lineages. ST1192 (former ST80) was the most prevalent, comprising 34 isolates (45.3%), followed by ST7 (former ST761) with 30 isolates (40.0%). Together, these 2 STs accounted for 64 of 75 isolates (85.3%). Temporal isolate detection mapping (Figure 1) revealed that ST7 predominated during 2022, whereas ST1192 emerged in late 2022 and became the dominant lineage from mid-2023 onwards, indicating a marked shift in clonal composition over the study period.

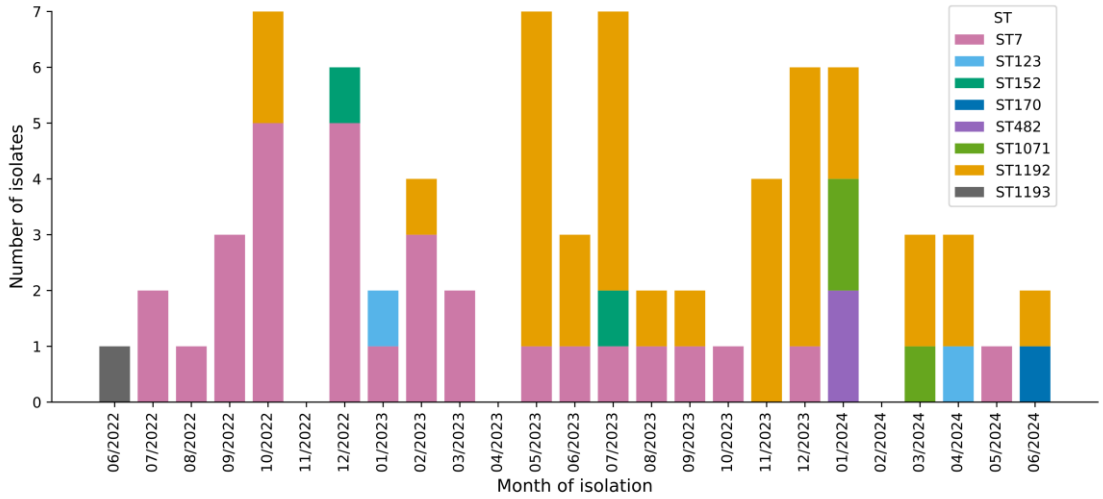


Figure 1. Temporal distribution of 75 *E. faecium* study isolates by sequence type (ST) from June 2022 to June 2024. Bars represent the number of isolates recovered per month.

To further investigate potential transmission events involving ST7 and ST1192, we examined patient hospitalization timelines in the hemato-oncology ward (Figure 2). Several patients exhibited overlapping hospital stays across clinical wards, suggesting opportunities for intra-hospital transmission. In one case, follow-up sampling yielded an isolate belonging to an ST different from the one detected initially, indicating strain replacement.

The remaining 11 isolates were distributed among 6 less common STs: ST123 (formerly ST117; n = 2), ST152 (formerly ST80/ST761; n = 2), ST170 (formerly ST80; n = 1), ST482 (formerly ST80; n = 2), ST1071 (formerly ST80; n = 3), and ST1193 (formerly ST117; n = 1). These STs were detected sporadically during the study period.

Core-genome SNV analysis identified 13,154 variable sites and revealed 2 major clusters corresponding to the predominant sequence types, ST7 and ST1192 (Figure 3). Isolates belonging to ST7 displayed greater genetic diversity, with pairwise SNV distances ranging from 0 to 74 SNVs. However, most ST7 isolates differed by fewer than 12 SNVs (median pairwise distance: 1 SNV), with the broader range driven by a single divergent isolate. In contrast, all 34 ST1192 isolates clustered tightly, with pairwise SNV distances ranging from 0 to 6 SNVs. This genetically homogeneous cluster was detected over an extended period, including before and after several months without detected cases.

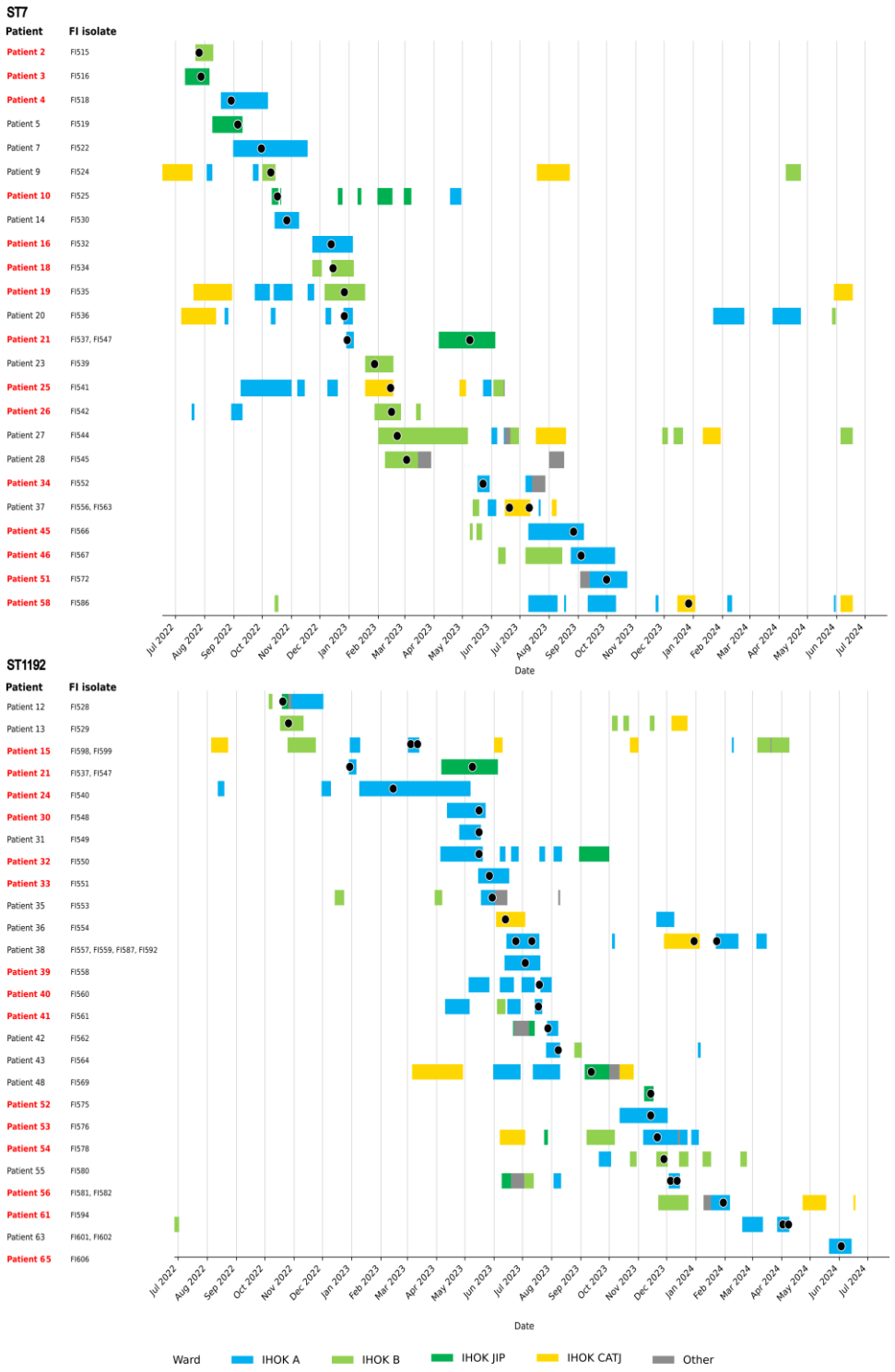


Figure 2. Hospitalization timelines of hemato-oncology patients. Colored bars indicate hospitalization periods at individual clinical departments, and black dots indicate collection of the study isolates. Patients highlighted in red received linezolid at some point during the study period; this designation does not necessarily indicate that treatment preceded isolate collection.

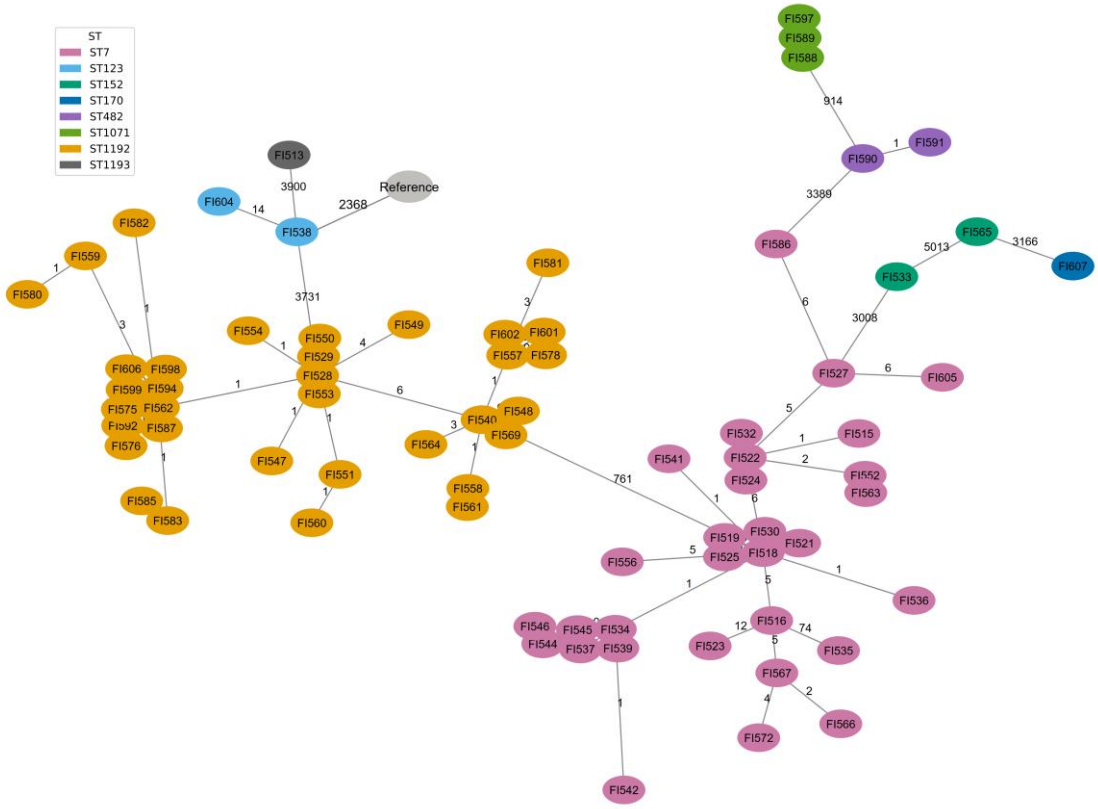


Figure 3. Minimum spanning tree of *E. faecium* isolates based on pairwise core-genome SNV distances. Each node represents an isolate and is colored according to sequence type. Numbers on connecting edges indicate the number of SNV differences between linked isolates. The tree was constructed using Kruskal's algorithm.

3.3. Phenotypic susceptibility and genetic resistance determinants

Confirmatory linezolid MICs were determined for all 75 study isolates and ranged from 4 to 256 mg/L. According to EUCAST clinical breakpoints (susceptible, ≤4 mg/L; resistant, >4 mg/L), 73 isolates were resistant to linezolid. Two isolates, FI547 and FI585, had an MIC of 4 mg/L and were therefore classified as susceptible despite having initially been reported as resistant by routine testing. The most frequently observed MIC was 256 mg/L (n = 20). All but 5 isolates were resistant to vancomycin.

Whole-genome sequencing identified the G2576T mutation in the 23S rRNA gene in all isolates, with mutant allele frequencies ranging from 2.8% to 98.0% (Supplementary Table S2). Ceiling-based estimates derived from these frequencies corresponded to 1 to 6 mutated 23S rRNA gene copies, with 62 isolates assigned to categories representing 3 or more copies (Table 1). Because these values were indirectly inferred from mutant allele frequencies, subsequent analyses were based on the measured frequencies. Neither plasmid-mediated linezolid-resistance genes (*optrA*, *poxtA*, and *cfr*) nor resistance-associated mutations in ribosomal protein genes (*rplC*, *rplD*, and *rplV*) were detected.

Table 1. Distribution of ceiling-based estimates of the number of 23S rRNA gene copies carrying the G2576T mutation. The estimated number of mutated copies was derived from the observed G2576T mutant allele frequency assuming six 23S rRNA gene copies per genome: Estimated number of mutated copies = ceiling [(mutant allele frequency/100) × 6]. The resulting categories represent indirect ceiling-based estimates rather than directly resolved individual 23S rRNA gene copies.

Estimated mutated-copy category (out of 6)	Number of isolates	Median MIC (mg/L)	Min MIC	Max MIC
1	2	8	8	8
2	11	16	6	48
3	16	24	12	256
4	16	56	6	256
5	11	128	4	256
6	19	256	4	256

We analyzed the relationships among linezolid MICs, G2576T mutant allele frequencies, sequence type, and documented linezolid treatment before isolate collection (Table 2 and Figure 4). The joint distribution of MICs and mutant allele frequencies showed substantial separation between the 2 predominant sequence types, with ST1192 isolates generally displaying higher values than ST7 isolates. In contrast, isolates with and without prior linezolid exposure overlapped extensively within both lineages. Across the complete collection, G2576T mutant allele frequency was positively correlated with linezolid MIC (Spearman's $\rho = 0.605$, $p < 0.000001$). The association remained significant within ST7 ($\rho = 0.512$, $p = 0.0038$), whereas a weaker, non-significant positive correlation was observed within ST1192 ($\rho = 0.255$, $p = 0.146$). These findings indicated that the overall association between mutant allele frequency and MIC was influenced in part by lineage structure rather than representing a uniform relationship across both predominant sequence types.



Figure 4. Relationship between linezolid MIC and G2576T mutant allele frequency among 75 *E. faecium* isolates. Each point represents one isolate. Colors indicate sequence type, and symbol shapes indicate documented linezolid treatment before isolate collection (circles, no prior treatment; triangles, prior treatment). Linezolid MIC values are displayed on a base-2 logarithmic scale. Points may overlap when isolates have identical or similar values.

Table 2. Linezolid MICs and G2576T mutant allele frequencies according to sequence type and documented linezolid treatment before isolate collection. Prior LZD denotes documented linezolid treatment before sampling; no prior LZD includes isolates collected before subsequent linezolid treatment and isolates from patients without documented linezolid treatment. MIC, minimum inhibitory concentration; IQR, interquartile range; LZD, linezolid.

	No prior LZD	Prior LZD	All
All isolates	38/75	37/75	75/75
MIC, median (mg/L)	32	48	32
G2576T, median (IQR), %	62.4 (49.3–83.7)	67.1 (48.0–96.1)	65.0 (48.6–86.3)
ST7	19/30	11/30	30/30
MIC, median (mg/L)	24	32	28
G2576T, median (IQR), %	50.2 (46.6–61.6)	54.6 (33.8–64.8)	50.3 (45.3–63.7)
ST1192	16/34	18/34	34/34
MIC, median (mg/L)	48	256	80
G2576T, median (IQR), %	83.2 (65.9–96.9)	96.4 (80.3–97.5)	86.3 (79.6–97.2)

Across the collection, isolates from patients with documented linezolid treatment before sampling had a higher median MIC than isolates without prior treatment (48 vs 32 mg/L), although the difference was not statistically significant (Mann–Whitney U = 813.5, $p = 0.235$). The two predominant sequence types, ST1192 and ST7, together accounted for 64 isolates and differed in their resistance characteristics. MICs were significantly higher in ST1192 than in ST7 (median, 80 vs 28 mg/L; Mann–Whitney U = 244.0, $p = 0.00026$; Hodges–Lehmann median difference, 32 mg/L; 95% CI, 10–192 mg/L). Within ST1192, isolates with documented linezolid treatment before sampling had a median MIC of 256 mg/L, compared with 48 mg/L among isolates without prior treatment; the difference was not statistically significant (Mann–Whitney U = 172.5, $p = 0.308$). Within ST7, the corresponding median MICs were 32 and 24 mg/L, respectively, with no statistically significant difference (Mann–Whitney U = 117.0, $p = 0.600$). ST1192 isolates had a significantly higher median G2576T mutant allele frequency than ST7 isolates (86.3% [IQR, 79.6–97.2%] vs 50.3% [IQR, 45.3–63.7%]; Mann–Whitney U = 86.5, $p < 0.000001$). Within ST1192, the median mutant allele frequency was 96.4% (IQR, 80.3–97.5%) among isolates with documented linezolid treatment before sampling and 83.2% (IQR, 65.9–96.9%) among isolates without prior treatment; the difference was not statistically significant (Mann–Whitney U = 180.0, $p = 0.220$). Within ST7, the corresponding values were 54.6% (IQR, 33.8–64.8%) and 50.2% (IQR, 46.6–61.6%), respectively, with no statistically significant difference (Mann–Whitney U = 105.0, $p = 1.000$). Across the collection, the corresponding median mutant allele frequencies were 67.1% (IQR, 48.0–96.1%) and 62.4% (IQR, 49.3–83.7%), respectively (Mann–Whitney U = 766.5, $p = 0.504$).

To account for repeated isolates from individual patients, a sensitivity analysis was performed using only the first chronologically collected isolate from each patient (n = 64; Table S3). The results were consistent with the primary analysis, with no statistically significant treatment-associated differences in MIC or G2576T mutant allele frequency across the full sensitivity-analysis cohort or within either predominant sequence type. Across all first isolates, median MICs were 48 and 32 mg/L

among isolates with and without prior linezolid treatment, respectively (Mann–Whitney U = 587.5, $p = 0.252$), while median mutant allele frequencies were 63.5% and 62.4% (Mann–Whitney U = 486.0, $p = 0.813$). Within ST7, the corresponding MICs were 32 and 28 mg/L (Mann–Whitney U = 110.0, $p = 0.632$), and mutant allele frequencies were 54.6% and 50.3% (Mann–Whitney U = 99.0, $p = 1.000$). Within ST1192, median MICs were 256 and 48 mg/L (Mann–Whitney U = 109.0, $p = 0.152$), whereas median mutant allele frequencies were 82.6% and 82.0% (Mann–Whitney U = 90.0, $p = 0.716$).

3.4. Plasmid diversity and distribution

Reconstruction of chromosomal and plasmid sequences identified a total of 500 plasmid contigs across all isolates, corresponding to a median of seven plasmids per isolate (range, 3–10). Plasmid phylogeny was reconstructed using PlasTree to assess the diversity and relatedness of plasmid sequences [25]. Plasmids carrying antimicrobial resistance and virulence genes were further characterized, and their distribution among isolates was investigated, with particular emphasis on the 2 dominant sequence types, ST7 and ST1192.

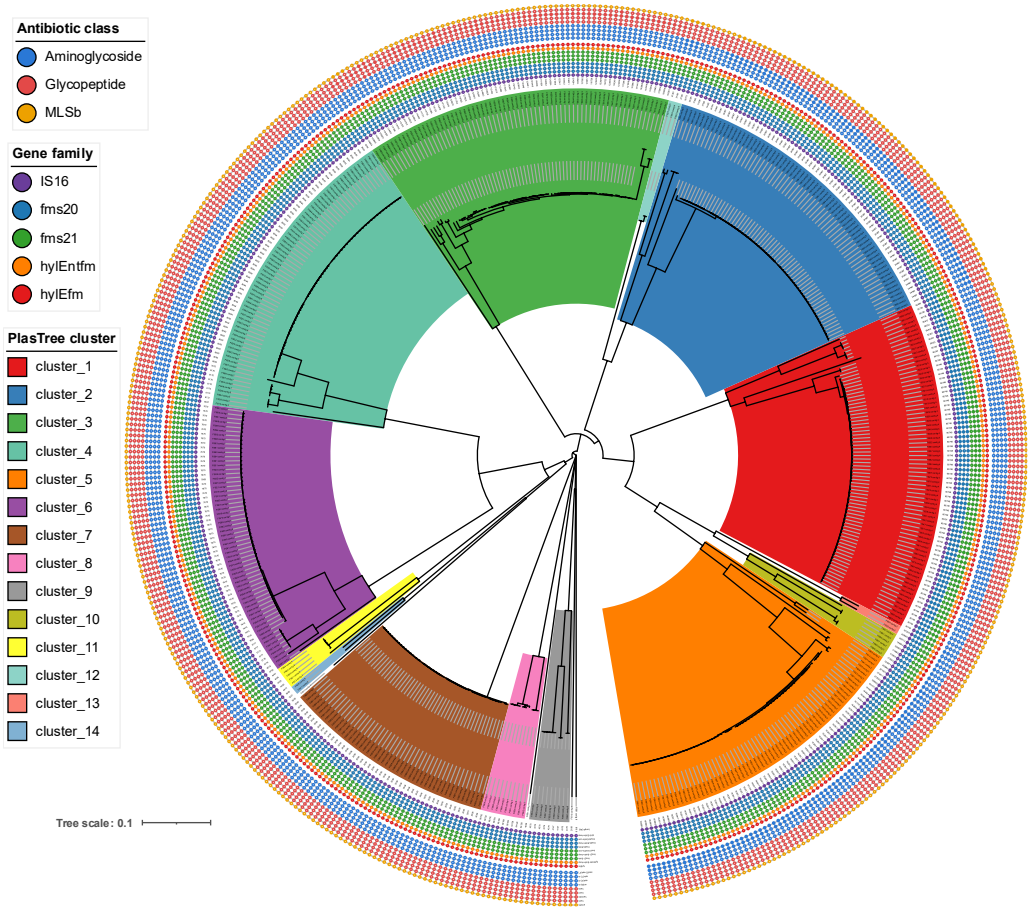


Figure 5. Sequence-similarity tree of 500 reconstructed plasmids from the study isolates. Terminal nodes represent individual plasmid sequences and are labeled according to the isolate identifier and plasmid contig number. Colors indicate assignment to PlasTree clusters 1–14. Tip symbols indicate antimicrobial resistance and virulence gene content, and the outer ring shows plasmid length.

PlasTree analysis assigned 496 plasmid contigs to 14 distinct clusters, while four contigs remained unclustered (Figure 5). None of the unclustered contigs carried identified antimicrobial resistance or putative virulence determinants. Among ST1192 isolates, clusters C1–C5 and C7 were present in all 34 isolates, C6 was detected in 32 isolates, and C9 in 3. Among ST7 isolates, C1 and C5 were present in all 30 isolates; C2 and C4 were each detected in 29 isolates, C3 in 28, C6 in 25, C7 in 10, C8 in 4, C9 in 3, C11 in 2, and C12 and C14 in 1 isolate each. Clusters C8, C11, C12, and C14 were detected in ST7 but not ST1192, whereas C10 and C13 were absent from both dominant lineages and occurred only among isolates belonging to less common sequence types.

Plasmids carrying antimicrobial resistance or putative virulence determinants were distributed across 6 PlasTree clusters (C1–C3, C5, C10, and C12). Differences in plasmid length within several clusters indicated structural variation among related plasmids, which was examined in greater detail for the pELF-like plasmids assigned to C3.

To compare complete plasmid repertoires, only isolates belonging to the 2 outbreak-associated sequence types (ST7 and ST1192; n = 64) were grouped into global plasmid profiles (GPs) based on the presence or absence of individual PlasTree clusters (Table 3). A total of 14 distinct GPs were identified. GP3 was the predominant profile, comprising 33 isolates, followed by GP1 with 13 isolates, whereas the remaining profiles were represented by 1 to 3 isolates each.

Table 3. Global plasmid profiles identified among outbreak-associated *E. faecium* isolates belonging to ST7 (n = 30) and ST1192 (n = 34). GP, global plasmid profile; C1–C14, PlasTree plasmid clusters; n, total number of isolates exhibiting the respective global plasmid profile. The presence and absence of individual plasmid clusters are indicated by √ and –, respectively.

GP	n	ST7	ST1192	C1	C2	C3	C4	C5	C6	C7	C8	C9	C10	C11	C12	C13	C14
GP1	13	13	0	√	√	√	√	√	√	–	–	–	–	–	–	–	–
GP2	1	1	0	√	√	√	√	√	√	√	–	–	–	√	–	–	–
GP3	33	4	29	√	√	√	√	√	√	√	–	–	–	–	–	–	–
GP4	1	1	0	√	√	–	√	√	√	–	–	–	–	–	–	–	–
GP5	1	1	0	√	√	√	√	√	√	√	–	√	–	√	√	–	–
GP6	1	1	0	√	√	√	–	√	√	√	–	√	–	–	–	–	–
GP7	1	1	0	√	–	–	√	√	–	–	–	–	–	–	–	–	–
GP8	1	1	0	√	√	√	√	√	√	√	–	–	–	–	–	–	√
GP9	1	1	0	√	√	√	√	√	√	√	√	–	–	–	–	–	–
GP10	3	0	3	√	√	√	√	√	√	√	–	√	–	–	–	–	–
GP11	2	0	2	√	√	√	√	√	–	√	–	–	–	–	–	–	–
GP12	2	2	0	√	√	√	√	√	√	–	√	–	–	–	–	–	–
GP13	1	1	0	√	√	√	√	√	–	√	√	√	–	–	–	–	–
GP14	3	3	0	√	√	√	√	√	–	–	–	–	–	–	–	–	–

The distribution of global plasmid profiles among the 2 dominant sequence types is shown in Figure 6. Among ST1192 isolates, 29 of 34 were assigned to GP3, while the remaining 5 belonged to GP10 (n = 3) or GP11 (n = 2). The 30 ST7 isolates comprised 12 global plasmid profiles. GP1 was the most common profile among ST7 isolates (13/30), whereas the remaining 17 isolates were distributed among 11 additional profiles.

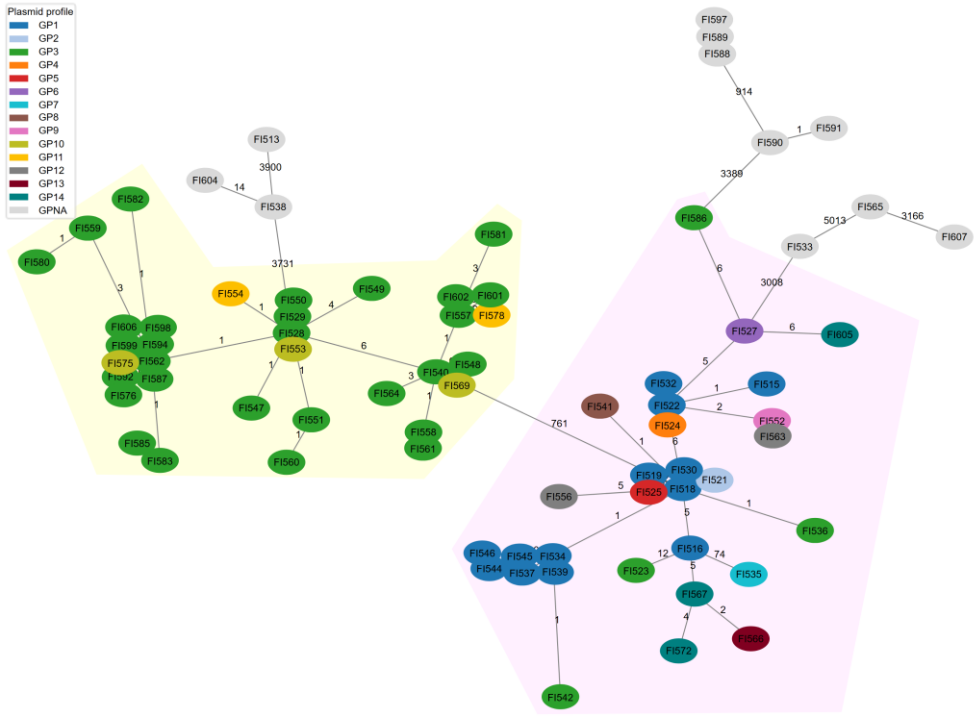


Figure 6. Minimum spanning tree (MST) illustrating clonal relationships among 75 *Enterococcus faecium* study isolates based on pairwise single nucleotide variant (SNV) distances. Each node represents a single isolate. Isolates belonging to the outbreak-associated sequence types (ST7 and ST1192) are colored according to their global plasmid profiles (GPs), whereas isolates of other sequence types are shown in grey. The ST7 and ST1192 clusters are highlighted by pink and yellow background shading, respectively. Numbers on connecting lines indicate SNV differences between neighbouring isolates.

Comparison of individual profiles showed that most differed from the predominant lineage-associated profiles by the gain or loss of only one or a few plasmids (Table 4). The dominant profiles GP1 and GP3 differed only by the presence of C7, which carried none of the antimicrobial resistance or putative virulence determinants listed in Table 5. Similarly, the minor ST1192 profiles GP10 and GP11 differed from GP3 by the acquisition of C9 or the loss of C6, respectively. These changes did not alter the listed antimicrobial resistance or putative virulence gene repertoire. Thus, much of the observed profile diversity reflected variation in accessory plasmids rather than major differences in known resistance or virulence determinants.

Several ST7 profiles nevertheless involved changes of direct clinical relevance. GP4 and GP7 lacked the pELF-like C3 plasmid carrying *vanHAX*. In the GP4 isolate FI524, *vanHAX* was on a C5 plasmid, whereas the GP7 isolate FI535 lacked *vanHAX* and was phenotypically susceptible to vancomycin. GP7 also lacked the C2 plasmid carrying *ant(6)-Ia*, *aph(3')-III*, and *erm(B)*. Conversely, GP5 contained an additional C12 plasmid carrying the same resistance gene combination as C2. These findings show that specific plasmid acquisition, loss, or relocation events altered the genomic context and, in some cases, the presence of clinically relevant resistance determinants.

The temporal distribution of global plasmid profiles reflected the changing composition of the outbreak population (Figure 7). Multiple profiles, predominantly associated with ST7, co-circulated during the early study period, whereas GP3 became increasingly predominant as ST1192 expanded. The continued detection of GP3 during the later study period suggests that the expansion of ST1192 occurred without major changes in its plasmid complement. Nevertheless, because GP3 was strongly associated with ST1192, its increasing frequency most likely accompanied the expansion of this lineage and does not independently demonstrate selection for the plasmid profile. Patient 21 illustrates this population shift: An ST7 isolate carrying GP1 was recovered during an earlier hospitalization, followed by an ST1192 isolate carrying GP3 during a subsequent admission. This observation is compatible with replacement of the original colonizing lineage or acquisition of a second outbreak-associated lineage.

Table 4. Differences in PlasTree cluster composition among global plasmid profiles (GP) and their potential functional relevance.

GP	n	Predominant ST	Difference from the lineage-associated reference profile	Potential functional relevance
GP1	13	ST7	Reference ST7 profile (C1–C6)	Carries the prevalent fms- and resistance-associated clusters C1, C2, C3, and C5
GP2	1	ST7	GP1 + C7 + C11	No additional determinants listed in Table 5
GP3	33	ST1192; ST7	GP1 + C7; reference ST1192 profile	C7 carried no listed resistance or putative virulence determinants
GP4	1	ST7	GP1 − C3	Loss of the pELF-like C3 plasmid; in FI524, vanHAX was located on C5
GP5	1	ST7	GP1 + C7 + C9 + C11 + C12	Additional C12 plasmid carrying ant(6)-Ia, aph(3′)-III, and erm(B)
GP6	1	ST7	GP1 − C4 + C7 + C9	No additional determinants listed in Table 5
GP7	1	ST7	GP1 − C2 − C3 − C6	Absence of the C2 resistance plasmid and the vanHAX-carrying C3 plasmid; FI535 was vancomycin susceptible
GP8	1	ST7	GP1 + C7 + C14	No additional determinants listed in Table 5
GP9	1	ST7	GP1 + C7 + C8	No additional determinants listed in Table 5
GP10	3	ST1192	GP3 + C9	No additional determinants listed in Table 5
GP11	2	ST1192	GP3 − C6	No additional determinants listed in Table 5
GP12	2	ST7	GP1 + C8	No additional determinants listed in Table 5
GP13	1	ST7	GP1 − C6 + C7 + C8 + C9	No additional determinants listed in Table 5
GP14	3	ST7	GP1 − C6	No additional determinants listed in Table 5

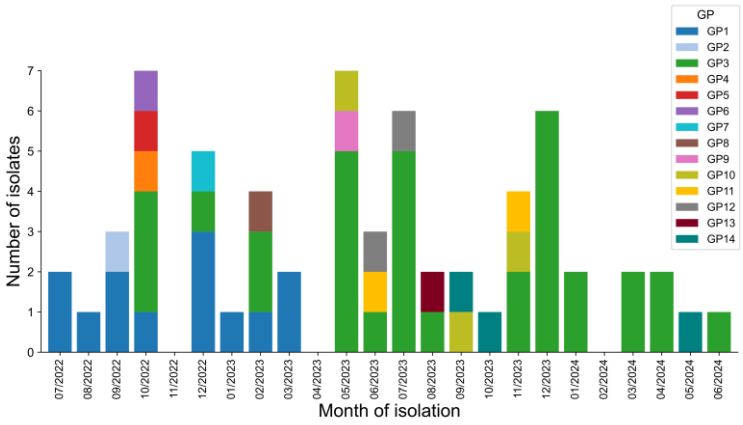


Figure 7. Temporal distribution of global plasmid profiles (GPs) among outbreak-associated *Enterococcus faecium* isolates. Stacked bar chart showing the number of isolates collected each month, with colors indicating the assigned global plasmid profiles. The figure illustrates changes in the distribution of plasmid profiles over the study period.

Following the analysis of global plasmid profiles, individual plasmid clusters carrying antimicrobial resistance or putative virulence genes were examined in greater detail (Table 5).

PlasTree cluster C3 corresponded to a pELF-like plasmid carrying the *vanHAX* operon and showed sequence similarity to the previously described plasmid pELF VR2 (PV113235.1). It was detected in all ST1192 isolates (34/34), 28 of 30 ST7 isolates, and 7 of the remaining 11 isolates. The reconstructed pELF-like plasmid lengths ranged from approximately 106 to 200 kbp.

The two ST7 isolates lacking the characteristic pELF-like plasmid differed in their *vanHAX* status. In isolate FI524, the *vanHAX* operon was on a different plasmid backbone assigned to cluster C5. In contrast, isolate FI535 lacked the pELF-like plasmid and the *vanHAX* operon and was phenotypically susceptible to vancomycin.

Four representative plasmids selected across this size distribution were compared to illustrate structural variation within cluster C3 (Figure 8). Differences in length were associated with partial or complete duplication of regions containing the *vanA* resistance gene cluster (*vanRSHAXYZ*), toxin–antitoxin systems, insertion sequences, and phage-associated genes. The extent of duplication varied among the representative plasmids, ranging from a single copy of the complete *vanA* gene cluster to partial duplication of its terminal *vanY–vanZ* region and duplication of the cluster.

Tn*1546-like* elements were identified in all 70 plasmids carrying the *vanHAX* gene cluster. The *vanH*, *vanA*, and *vanX* genes were complete in all plasmids, whereas the complete *vanRSHAXYZ* gene cluster was present in 69 plasmids. None of the elements contained the transposase gene *orf1*. The 69 pELF-like plasmids assigned to C3 were linear and classified as non-mobilizable, whereas the *vanHAX*-carrying plasmid in FI524 belonged to the circular, non-mobilizable C5 cluster. Three structural profiles were distinguished (Figure S1; Table S4). Profile P1 was detected in 66 plasmids from ST1192 (n = 34), ST7 (n = 29), ST482 (n = 2), and ST152 (n = 1). Its organization matched the previously described BC2-type structure, with IS*1216E*-associated disruption of *orf2*, IS*1251* inserted between *vanS* and *vanH*, and the T7658C and G8234T substitutions in *vanA* and *vanX*, respectively. Profile P2 was identified in all three ST1071 plasmids and differed from P1 by an additional IS*1216E* insertion between *vanX* and *vanY*. Profile P3 was detected in one ST123 plasmid and lacked *vanR* and

most of *vanS*, which were replaced by IS*1216E*; it also contained an IS*1216E* insertion between *vanX* and *vanY* and lacked IS*1251*. P1 therefore corresponded to the published BC2-type organization, whereas P2 and P3 did not correspond exactly to the published structures examined here and were retained as study-specific profiles.

Table 5. Characteristics of plasmid clusters identified using PlasTree.

PlasTre cluster	n	Circular?	Modal length (bp)	Mobility	STs	Virulence/Resistance genes (≥90% prevalence)	Closest BLAST match (accession)
C1	74	Yes	60748	conjugative	7; 1192; 123; 152; 170; 482; 1071	*fms20-Entfm-hosp; fms20-Entls*	CP111744.1
C2	70	Yes	24967	non-mobilizable	7; 1192; 123; 152; 482; 1071	*ant(6)-Ia; aph(3')-III; erm(B)*	CP064052.1
C3	69	No	118503	non-mobilizable	7; 1192; 123; 152; 482; 1071	*VanHAX*	PV113235.1
C4	69	Yes	8063	mobilizable	7; 1192; 123; 152; 170; 1193	ND	CP111510.1
C5	67	Yes	182917	non-mobilizable	7; 1192; 152; 1193	*aac(6')-aph(2"); aph(2")-Ia*	CP013995.1
C6	62	Yes	7670	non-mobilizable	7; 1192; 123; 152; 482	ND	CP175419.1
C7	48	Yes	2056	mobilizable	7; 1192; 123; 152; 482	ND	CP040707.1
C8	10	Yes	NA	conjugative	7; 170; 482; 1071	ND	CP197042.1
C9	9	Yes	4375	mobilizable	7; 1192; 152; 482	ND	CP063603.1
C10	6	Yes	175935	non-mobilizable	170; 482; 1071	*aac(6')-aph(2")*	CP023424.1
C11	5	Yes	4465	non-mobilizable	7; 123; 152; 1193	ND	CP044279.1
C12	3	Yes	27361	non-mobilizable	7; 123	*ant(6)-Ia; aph(3')-III; erm(B)*	CP064052.1
C13	2	Yes	NA	conjugative/non-mobilizable	123	ND	CP023424.1
C14	2	Yes	33221	non-mobilizable	7;123	ND	CP111885.1

Besides the pELF-like plasmid assigned to cluster C3, five additional plasmid clusters carrying antimicrobial resistance or putative virulence determinants were identified. Cluster C1 comprised 74 conjugative plasmids carrying the putative virulence-associated genes *fms20-Entfm-hosp* and *fms20-Entls*. These plasmids were detected across sequence types and showed high sequence similarity to CP111744.1. Cluster C2 included 70 non-mobilizable plasmids carrying *ant(6)-Ia*, *aph(3')-III*, and *erm(B)* and was detected across several sequence types; the closest BLAST match was CP064052.1. Cluster C5 comprised 67 non-mobilizable plasmids carrying *aac(6')-aph(2")* and *aph(2")-Ia*, with sequence similarity to CP013995.1. Cluster C10 consisted of 6 non-mobilizable plasmids carrying *aac(6')-aph(2")* and was detected in ST170, ST482, and ST1071; its closest match was CP023424.1.

Finally, cluster C12 comprised three non-mobilizable plasmids from ST7 and ST123 carrying *ant(6)-Ia*, *aph(3')-III*, and *erm(B)* and was also most closely related to CP064052.1.

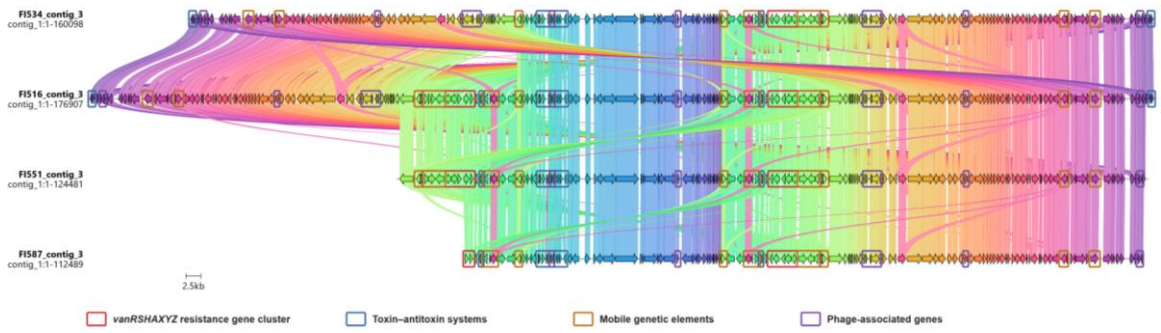


Figure 8. Comparative analysis of four representative pELF-like plasmids selected across the continuous distribution of reconstructed plasmid lengths. Coding sequences are shown as arrows, with homologous genes displayed in matching colors, while shaded links indicate regions of sequence similarity. Colored boxes highlight the *vanA* resistance gene cluster (*vanRSHAXYZ*; red), toxin–antitoxin systems (blue), mobile genetic elements (orange), and phage-associated genes (purple). Differences in plasmid length reflect variable partial or complete duplication of regions containing these genetic determinants. The displayed plasmids represent examples from the observed size continuum rather than discrete structural groups. A fully annotated version of the figure, including individual gene labels, is shown in Supplementary Figure S3.

4. Discussion

This study provides a genomic and phenotypic characterization of *E. faecium* isolates initially identified as linezolid resistant during routine laboratory testing and collected over a two-year period at a single tertiary-care hospital. The predominance of 2 clonal lineages, ST1192 and ST7, aligns with the population structure of hospital-adapted *E. faecium*, in which locally successful lineages may emerge and expand through clonal transmission, recombination, acquisition of mobile genetic elements, and antimicrobial selection [31,32]. Their prolonged detection supports sustained circulation within the institution, although the available sampling cannot distinguish continuous transmission from persistence in unsampled reservoirs or repeated reintroduction.

The 2 dominant lineages displayed distinct patterns of genomic diversity and temporal occurrence. ST7 showed greater overall diversity, with pairwise SNV distances ranging from 0 to 74 SNVs, although the median pairwise distance was 1 SNV and most isolates differed by fewer than 12 SNVs. The wider range was driven by a single divergent isolate and may reflect the coexistence of multiple related sublineages, repeated introductions, or transmission from a persistent reservoir. In contrast, ST1192 formed a genetically homogeneous cluster, with pairwise distances of 0–6 SNVs, suggesting recent common ancestry and limited diversification. Detection of ST1192 before and after several months without identified cases is compatible with prolonged patient colonization, an unsampled environmental or patient reservoir, or undetected transmission, patterns previously described in hospital-associated *E. faecium* populations [31,33].

Application of the MLST scheme proposed by Bezdíček et al. provided improved differentiation of the study population compared with the original Homan scheme [15,16]. Isolates previously assigned to the same sequence types were separated into genetically more coherent groups, facilitating interpretation of the population structure observed by higher-resolution genomic analyses. Nevertheless, MLST remains a typing framework with substantially lower resolution than cgMLST or SNV-based analysis and should not be used alone to infer recent transmission.

To place our findings in a broader genomic context, we compared the study isolates with 3,278 publicly available *E. faecium* genomes from PubMLST using cgMLST and the MLST scheme proposed by Bezdíček et al. [16]. The comparison is illustrated in Supplementary Figure S2. The closest publicly available genomes originated from Pakistan, Norway, India, Spain, and Ireland, but differed from the study isolates by at least 28 cgMLST alleles. ST1192 and ST7 formed compact clusters within the broader dataset and remained distinct from internationally distributed lineages such as ST4 (formerly ST1421), ST17 (formerly ST117), ST143 (formerly ST80), and ST133 (formerly ST18) [31,33]. Because the PubMLST collection is geographically and temporally uneven and was not selected for linezolid resistance, this comparison is descriptive rather than epidemiological. It supports genetic distinctness within the analyzed dataset but cannot exclude unsampled introductions or undocumented transmission.

The G2576T mutation in the 23S rRNA gene, a well-established mechanism of linezolid resistance [7,34], was detected in all isolates. Its presence in the 2 isolates classified as susceptible by confirmatory MIC testing is consistent with reports that resistance-associated mutations or genes may occur in phenotypically susceptible enterococci [35]. ST1192 showed higher G2576T mutant allele frequencies and higher linezolid MICs than ST7. Across the complete collection, mutant allele frequency was positively correlated with MIC, consistent with the established gene-dosage effect whereby increasing proportions of mutated 23S rRNA gene copies are associated with higher linezolid MICs [34,36]. However, the association was not uniform across lineages: It remained significant within ST7 but was weaker and non-significant within ST1192. The overall correlation therefore appears to reflect within-lineage variation and differences between the predominant lineages. Nevertheless, documented treatment before sampling did not show a uniform association with either MIC or mutant allele frequency across the complete collection. No acquired linezolid-resistance determinants (*optrA*, *poxtA*, or *cfr*) were detected, despite their documented dissemination across clinical, animal, and environmental settings [9,37,38]. Horizontal transfer of these known determinants therefore did not contribute detectably to linezolid resistance in this cohort.

Of the 75 isolates, 37 were collected after documented linezolid treatment, whereas 38 (50.7%) were collected before any documented treatment. This indicates that the observed lineages were not restricted to patients with documented linezolid exposure and may have circulated more broadly within the hospital. However, because treatment data were collected retrospectively, these findings cannot distinguish transmission from undetected colonization or exclude undocumented prior exposure. Across the complete collection, the median MIC was higher among isolates with prior treatment than among those without prior treatment (48 vs 32 mg/L), although the difference was not statistically significant. Within ST1192, the median MIC was numerically higher among isolates with prior treatment than among those without prior treatment (256 vs 48 mg/L), whereas the corresponding medians within ST7 were 32 and 24 mg/L. Neither within-lineage comparison was statistically significant.

G2576T mutant allele frequencies were numerically higher among isolates from patients with prior linezolid treatment than among those without prior treatment overall (67.1% vs 62.4%) and within ST1192 (96.4% vs 83.2%), whereas the difference within ST7 was smaller (54.6% vs 50.2%). None of the treatment-related comparisons were statistically significant in the isolate-level analysis or in the first-isolate sensitivity analysis. Overall, the data do not demonstrate a reproducible association between documented linezolid treatment before sampling and either MIC or G2576T mutant allele frequency across the collection.

Because no acquired linezolid-resistance genes or additional established resistance-associated mutations were detected, the difference in MICs between ST1192 and ST7 may partly reflect their different G2576T mutant allele frequencies. Contributions from other lineage-specific genomic factors cannot be excluded, and the close association between sequence type and mutant allele frequency prevented their independent effects from being determined. In addition, the number of 23S rRNA gene copies carrying G2576T was inferred indirectly from mutant allele frequencies and was not confirmed by copy-specific sequencing or another experimental method. Allele-frequency estimates may be affected by sequencing, basecalling, and read-mapping variation, particularly at low frequencies. The derived copy-number categories should therefore be interpreted cautiously, and the principal genotype–phenotype analyses were appropriately based on the observed mutant allele frequencies.

Long-read sequencing revealed shared and lineage-associated features of the plasmidome. ST1192 and ST7 shared several prevalent PlasTree clusters, which may reflect stable vertical maintenance, exchange between co-circulating lineages, or repeated acquisition from a shared plasmid pool. Global plasmid profiling nevertheless showed different degrees of heterogeneity between the lineages. The predominance of GP3 and closely related variants within ST1192 suggested maintenance of a largely conserved plasmid complement during clonal expansion, whereas the greater number of profiles within ST7 paralleled its higher chromosomal diversity. The temporal increase in GP3 largely accompanied the expansion of ST1192 and should not be interpreted as independent evidence of selection for this plasmid profile.

The pELF-like C3 plasmid was widely distributed and was not restricted to a single chromosomal lineage, as reported for pELF-type plasmids in multidrug-resistant *E. faecium* populations [4,39]. Its distribution could reflect vertical inheritance, horizontal dissemination, or both; these possibilities cannot be distinguished without experimental transfer data. The continuous distribution of reconstructed plasmid lengths and the presence of insertion sequences within or adjacent to structurally variable regions are consistent with a role for mobile genetic elements in pELF-like plasmid plasticity [3,4]. The two ST7 exceptions further showed that *vanHAX* was not invariably associated with the C3 backbone and could occur on an alternative C5 plasmid or be absent.

The Tn*1546-like* analysis further placed these findings in the context of previously described *vanA* plasmid systems. A Czech study of vancomycin-resistant *E. faecium* ST117 identified BC2-type Tn*1546* on pELF2-like plasmids, whereas a study from Dallas described multiple Tn*1546* structures on pRUM-like plasmids [40,41]. In our collection, the BC2-type P1 profile was predominantly associated with the pELF-like C3 plasmid but was also present on the alternative C5 backbone in FI524. This observation supports the interpretation that a conserved Tn*1546* structure may occur in different plasmid contexts and across chromosomal lineages. The additional P2 and P3 profiles indicate local structural diversification of the resistance element. Because published Tn*1546* nomenclature is not fully standardized, we retain the study-specific profile labels P1-P3 in addition to the BC2 designation for P1.

Other plasmid clusters carried resistance determinants or putative colonization-associated factors. The nearly ubiquitous conjugative C1 plasmid carried *fms20*-associated genes and was detected across sequence types. C2 and C5 were also broadly distributed and comprised non-mobilizable plasmids carrying, respectively, *ant(6)-Ia*, *aph(3')-III*, and *erm(B)*, or *aac(6')-aph(2")* and *aph(2")-Ia*. Their broad distribution may reflect stable maintenance within successful lineages, although mobilization mediated by co-resident conjugative elements cannot be excluded. The less frequent C10 and C12 clusters demonstrated that related resistance determinants also occurred in distinct plasmid backgrounds: C10 carried *aac(6')-aph(2")*, whereas C12 carried the same *ant(6)-Ia*, *aph(3')-III*, and *erm(B)* combination as C2. The C1 *fms20*-associated genes have been linked to gut colonization and virulence in *E. faecium* [42], but experimental studies would be required to determine whether this plasmid contributed to adhesion, persistence, or horizontal dissemination in the study population.

Overall, the plasmid analyses revealed a combination of stability and structural plasticity. Major resistance-associated plasmid clusters were broadly conserved, whereas differences among global plasmid profiles mainly involved a limited number of accessory plasmids. Furthermore, structural variation among pELF-like plasmids and detection of *vanHAX* on an alternative plasmid backbone illustrate how resistance determinants may be maintained despite changes in plasmid architecture [4,39]. These findings complement the chromosomal analysis by showing that closely related isolates may differ in plasmid composition, whereas distinct chromosomal lineages may share related plasmid elements, as observed in population-level genomic studies [3,9]. Because environmental sampling, systematic longitudinal sampling, and experimental transfer studies were not performed, the direction and mechanisms of plasmid dissemination within the hospital could not be determined.

This study has several additional limitations. Multiple isolates were available from some patients, although a first-isolate sensitivity analysis was performed. Treatment information was collected retrospectively, and although treatment timing and duration were available, this analysis used only a binary indicator of documented treatment before sampling and did not account for cumulative dose and treatment duration; this exposure heterogeneity limited causal interpretation. SNV analyses were based on long-read sequencing and were therefore interpreted conservatively, while the inferred numbers of mutated 23S rRNA gene copies were not experimentally confirmed. These limitations should be considered when interpreting transmission patterns, treatment associations, and plasmid dissemination.

In conclusion, in this single-centre study, we identified 2 predominant G2576T-positive *E. faecium* lineages with contrasting patterns of genomic diversity. Higher G2576T mutant allele frequencies in ST1192 coincided with higher linezolid MICs, whereas documented linezolid exposure before sampling did not show a uniform association with either measure. Long-read sequencing revealed a broadly shared plasmid repertoire, lineage-associated differences in global plasmid profiles, and extensive structural variation among pELF-like plasmids carrying the *vanA* resistance gene cluster. Together, these findings demonstrate the complementary value of chromosomal and plasmid analyses for understanding the persistence and evolution of hospital-associated *E. faecium*. Genomic surveillance incorporating both components may improve recognition of emerging lineages, resistance evolution, and changes in plasmid-mediated resistance relevant to infection control and antimicrobial stewardship.

Use of AI tools declaration

During the preparation of this manuscript, the authors used ChatGPT (OpenAI) for language editing and to assist with preparing Python code for figure generation and R code for statistical analyses. All AI-assisted outputs were reviewed and verified by the authors, who take full responsibility for the final content, analyses, and conclusions.

Ethics statement

This study used bacterial isolates obtained during routine clinical microbiology diagnostics at University Hospital Brno. The Ethics Committee of University Hospital Brno did not require ethical approval because the study involved only microbial cultures collected during routine diagnostics and pseudonymized data without any direct patient identifiers.

Data availability

Assembled genome sequences and reconstructed plasmid sequences for all study isolates, with consistent isolate identifiers and corresponding linezolid MIC values, are available from Zenodo at https://doi.org/10.5281/zenodo.23369716. Raw sequencing reads are available in the NCBI Sequence Read Archive under accession numbers SRR39545816–SRR39545845 and SRR40037740–SRR40037784 (BioProject PRJNA675431).

Acknowledgements

This study was supported by Czech Health Research Council (Grant No. NW24-09-00126); Ministry of Health, Czech Republic—conceptual development of research organization (FNBr, 65269705); and Masaryk University (MUNI/A/1733/2025).

Conflict of interest

The authors declare that the research was conducted in the absence of any commercial or financial relationships that could be construed as a potential conflict of interest.

Author contributions

H. E.: Writing—original draft, Formal analysis, Conceptualization, Investigation, Methodology. J. M.: Software, Writing—original draft, Formal analysis, Visualization, Data curation, Validation. B. M.: Methodology, Writing—review & editing, Investigation. B. V.: Writing—review & editing, Methodology, Investigation. V. H.: visualization, Software, Data curation, Writing—review & editing. K. I.: Methodology, Writing—review & editing, Resources. V. I.: Resources, Writing—review & editing, Methodology. K. P.: Resources, Writing—review & editing, Methodology; K. T.: Methodology, Writing—review & editing, Resources. W. B.: Methodology, Writing—review & editing, Resources. H.S.: Methodology, Writing—review & editing, Resources. Z. D. L.: Resources, Writing—review & editing, Funding acquisition. L. M.: Investigation, Validation, Writing—review & editing, Resources, Funding acquisition, Writing—original draft, Project administration.

References

1. Fisher K, Phillips C (2009) The ecology, epidemiology and virulence of *Enterococcus*. *Microbiol* 155: 1749–1757. https://doi.org/10.1099/mic.0.026385-0
2. Phyo Thu W, Sinwat N, Chuanchuen R (2018) Plasmid profile of *Enterococcus faecium* and *Enterococcus faecalis* isolated from pigs, pork and humans in Thai-Laos border provinces. *Thai J Vet Med* 48: 623–630. https://doi.org/10.56808/2985-1130.2954
3. Arredondo-Alonso S, Top J, McNally A, et al. (2020) Plasmids shaped the recent emergence of the major nosocomial pathogen *Enterococcus faecium*. *mBio* 11: e03284-19. https://doi.org/10.1128/mbio.03284-19
4. Hashimoto Y, Suzuki M, Kobayashi S, et al. (2023) Enterococcal linear plasmids adapt to *Enterococcus faecium* and spread within multidrug-resistant clades. *Antimicrob Agents Chemother* 67: e01619-22. https://doi.org/10.1128/aac.01619-22
5. Wei Y, Palacios Araya D, Palmer KL (2024) *Enterococcus faecium*: Evolution, adaptation, pathogenesis and emerging therapeutics. *Nat Rev Microbiol* 22: 705–721. https://doi.org/10.1038/s41579-024-01058-6
6. Mališová L, Jakubů V, Pomorská K, et al. (2021) Spread of linezolid-resistant *Enterococcus spp*. in human clinical isolates in the Czech Republic. *Antibiotics* 10: 219. https://doi.org/10.3390/antibiotics10020219
7. Long KS, Vester B (2012) Resistance to linezolid caused by modifications at its binding site on the ribosome. *Antimicrob Agents Chemother* 56: 603–612. https://doi.org/10.1128/aac.05702-11
8. Wang Y, Lv Y, Cai J, et al. (2015) A novel gene, *optrA*, that confers transferable resistance to oxazolidinones and phenicols and its presence in *Enterococcus faecalis* and *Enterococcus faecium* of human and animal origin. *J Antimicrob Chemother* 70: 2182–2190. https://doi.org/10.1093/jac/dkv116
9. Egan SA, Shore AC, O'Connell B, et al. (2020) Linezolid resistance in *Enterococcus faecium* and *Enterococcus faecalis* from hospitalized patients in Ireland: high prevalence of the MDR genes *optrA* and *poxtA* in isolates with diverse genetic backgrounds. *J Antimicrob Chemother* 75: 1704–1711. https://doi.org/10.1093/jac/dkaa075
10. Li H (2018) Minimap2: Pairwise alignment for nucleotide sequences. *Bioinformatics* 34: 3094–3100. https://doi.org/10.1093/bioinformatics/bty191
11. Wick RR, Howden BP, Stinear TP (2025) Autocycler: Long-read consensus assembly for bacterial genomes. *Bioinformatics* 41: btaf474. https://doi.org/10.1093/bioinformatics/btaf474
12. Kolmogorov M, Yuan J, Lin Y, et al. (2019) Assembly of long, error-prone reads using repeat graphs. *Nat Biotechnol* 37: 540–546. https://doi.org/10.1038/s41587-019-0072-8
13. Li H (2016) Minimap and miniasm: Fast mapping and *de novo* assembly for noisy long sequences. *Bioinformatics* 32: 2103–2110. https://doi.org/10.1093/bioinformatics/btw152
14. Vaser R, Sikic M (2021) Time- and memory-efficient genome assembly with Raven. *Nat Comput Sci* 1: 332–336. https://doi.org/10.1038/s43588-021-00073-4
15. Homan WL, Tribe D, Poznanski S, et al. (2002) Multilocus sequence typing scheme for *Enterococcus faecium*. *J Clin Microbiol* 40: 1963–1971. https://doi.org/10.1128/JCM.40.6.1963-1971.2002

16. Bezdicek M, Hanslikova J, Nykrynova M, et al. (2023) New multilocus sequence typing scheme for *Enterococcus faecium* based on whole genome sequencing data. *Microbiol Spectr* 11: e05107-22. https://doi.org/10.1128/spectrum.05107-22
17. Seemann T. Snippy: Rapid haploid variant calling and core genome alignment. GitHub. Available from: https://github.com/tseemann/snippy.
18. Kruskal JB (1956) On the shortest spanning subtree of a graph and the traveling salesman problem. *Proc Am Math Soc* 7: 48–50. https://doi.org/10.1090/S0002-9939-1956-0078686-7
19. Shannon P, Markiel A, Ozier O, et al. (2003) Cytoscape: A software environment for integrated models of biomolecular interaction networks. *Genome Res* 13: 2498–2504. https://doi.org/10.1101/gr.1239303
20. Florensa AF, Kaas RS, Clausen PTLC, et al. (2022) ResFinder—an open online resource for identification of antimicrobial resistance genes in next-generation sequencing data and prediction of phenotypes from genotypes. *Microb Genom* 8: 000748. https://doi.org/10.1099/mgen.0.000748
21. Joensen KG, Scheutz F, Lund O, et al. (2014) Real-time whole-genome sequencing for routine typing, surveillance, and outbreak detection of verotoxigenic *Escherichia coli*. *J Clin Microbiol* 52: 1501–1510. https://doi.org/10.1128/JCM.03617-13
22. Hasman H, Clausen PTLC, Kaya H, et al. (2019) LRE-Finder, a Web tool for detection of the 23S rRNA mutations and the *optrA*, *cfr*, *cfr(B)* and *poxtA* genes encoding linezolid resistance in enterococci from whole-genome sequences. *J Antimicrob Chemother* 74: 1473–1476. https://doi.org/10.1093/jac/dkz092
23. Camacho C, Coulouris G, Avagyan V, et al. (2009) BLAST+: Architecture and applications. *BMC Bioinformatics* 10: 421. https://doi.org/10.1186/1471-2105-10-421
24. Qin X, Galloway-Pena JR, Sillanpaa J, et al. (2012) Complete genome sequence of *Enterococcus faecium* strain TX16 and comparative genomic analysis of *Enterococcus faecium* genomes. *BMC Microbiol* 12: 135. https://doi.org/10.1186/1471-2180-12-135
25. BioSys-BUT (2026) PlasTree. GitHub. Available from: https://github.com/BioSys-BUT/PlasTree.
26. Schwengers O, Jelonek L, Dieckmann MA, et al. (2021) Bakta: Rapid and standardized genome annotation for bacteria. *Microb Genom* 7: 000685. https://doi.org/10.1099/mgen.0.000685
27. Tonkin-Hill G, MacAlasdair N, Ruis C, et al. (2020) Producing polished prokaryotic pangenomes with the Panaroo pipeline. *Genome Biol* 21: 180. https://doi.org/10.1186/s13059-020-02090-4
28. Robertson J, Nash JHE (2018) MOB-suite: Software tools for clustering, reconstruction and typing of plasmids from draft assemblies. *Microb Genom* 4: e000206. https://doi.org/10.1099/mgen.0.000206
29. Arthur M, Molinas C, Depardieu F, et al. (1993) Characterization of Tn*1546*, a Tn3-related transposon conferring glycopeptide resistance by synthesis of depsipeptide peptidoglycan precursors in Enterococcus faecium BM4147. *J Bacteriol* 175: 117–127. https://doi.org/10.1128/jb.175.1.117-127.1993
30. Siguier P, Perochon J, Lestrade L, et al. (2006) ISfinder: The reference centre for bacterial insertion sequences. *Nucleic Acids Res* 34: D32–D36. https://doi.org/10.1093/nar/gkj014
31. Raven KE, Gouliouris T, Brodrick H, et al. (2017) Complex routes of nosocomial vancomycin-resistant *Enterococcus faecium* transmission revealed by genome sequencing. *Clin Infect Dis* 64: 886–893. https://doi.org/10.1093/cid/ciw872
32. van Hal SJ, Willems RJL, Gouliouris T, et al. (2021) The global dissemination of hospital clones of *Enterococcus faecium*. *Genome Med* 13: 52. https://doi.org/10.1186/s13073-021-00868-0

33. Segawa T, Masuda K, Hisatsune J, et al. (2024) Genomic analysis of inter-hospital transmission of vancomycin-resistant *Enterococcus faecium* sequence type 80 isolated during an outbreak in Hiroshima, Japan. *Antimicrob Agents Chemother* 68: e01716-23. https://doi.org/10.1128/aac.01716-23
34. Schnitzler P, Schulz K, Lampson C, et al. (2011) Molecular analysis of linezolid resistance in clinical *Enterococcus faecium* isolates by polymerase chain reaction and pyrosequencing. *Eur J Clin Microbiol Infect Dis* 30: 121–125. https://doi.org/10.1007/s10096-010-1046-4
35. Bender JK, Fleige C, Funk F, et al. (2024) Linezolid resistance genes and mutations among linezolid-susceptible *Enterococcus spp*.—A loose cannon? *Antibiotics* 13: 101. https://doi.org/10.3390/antibiotics13010101
36. Marshall SH, Donskey CJ, Hutton-Thomas R, et al. (2002) Gene dosage and linezolid resistance in *Enterococcus faecium* and *Enterococcus faecalis*. *Antimicrob Agents Chemother* 46: 3334–3336. https://doi.org/10.1128/AAC.46.10.3334-3336.2002
37. Wang Z, Liu D, Zhang J, et al. (2024) Genomic epidemiology reveals multiple mechanisms of linezolid resistance in clinical enterococci in China. *Ann Clin Microbiol Antimicrob* 23: 41. https://doi.org/10.1186/s12941-024-00689-0
38. Shen W, Cai C, Dong N, et al. (2024) Mapping the widespread distribution and transmission dynamics of linezolid resistance in humans, animals, and the environment. *Microbiome* 12: 52. https://doi.org/10.1186/s40168-023-01744-2
39. Hashimoto Y, Dao DT, Kasuga I, et al. (2025) Ongoing independent evolution of linezolid and vancomycin-resistance pELF-type linear plasmids across the One Health spectrum. *Antimicrob Agents Chemother* 69: e01168-25. https://doi.org/10.1128/aac.01168-25
40. Brajerova M, Nyc O, Drevinek P, et al. (2025) Genomic insights into the spread of vancomycin- and tigecycline-resistant *Enterococcus faecium* ST117. *Ann Clin Microbiol Antimicrob* 24: 36. https://doi.org/10.1186/s12941-025-00806-7
41. Islam M, Sharon B, Abaragu A, et al. (2023) Vancomycin resistance in *Enterococcus faecium* from the Dallas, Texas, area is conferred predominantly on pRUM-like plasmids. *mSphere* 8: e00024-23. https://doi.org/10.1128/msphere.00024-23
42. Kim DS, Singh KV, Nallapareddy SR, et al. (2010) The *fms21 (pilA)-fms20* locus encoding one of four distinct pili of *Enterococcus faecium* is harboured on a large transferable plasmid associated with gut colonization and virulence. *J Med Microbiol* 59: 505–507. https://doi.org/10.1099/jmm.0.016238-0



AIMS Press

© 2026 the Author(s), licensee AIMS Press. This is an open access article distributed under the terms of the Creative Commons Attribution License (https://creativecommons.org/licenses/by/4.0)